

# Digital Predistortion of Power Amplifier Non-Linearities for Full-Duplex Transceivers

Andrew C. M. Austin, Alexios Balatsoukas-Stimming and Andreas Burg

Telecommunication Circuits Laboratory, École Polytechnique Fédérale de Lausanne, 1015 Lausanne, Switzerland

Email: andrew.austin@epfl.ch

**Abstract**—Non-linearities introduced by the power amplifier stage can significantly reduce the performance of self-interference cancellation in full-duplex transceivers. Accordingly, we propose a full-duplex system architecture that predistorts the digital baseband transmit signal to account for the non-linear memory effects of the power amplifier. Implementation results for a 5 MHz OFDM signal (operating with 20 dBm average transmit power) on a full-duplex testbed show that a further 13 dB suppression can be obtained, compared to the case when no predistortion is applied. The power levels of out-of-band emissions are also significantly reduced.

**Index Terms**—Full-Duplex, Digital Predistortion, Power Amplifier, Non-Linear Modelling.

## I. INTRODUCTION

The limited availability of suitable radio frequency (RF) spectrum has renewed interest in physical-layer technologies to improve spectral efficiency. One of the most promising techniques is full-duplex communication, where transmission and reception can occur simultaneously in the same frequency band [1]. The practical realisation of such systems requires the strong self-interference signal (arising from the closely coupled transmitter and receiver circuits) to be suppressed, ideally to the noise-floor, as any residual self-interference will reduce the signal-to-noise ratio of the incoming desired signal. Suppression of the self-interference typically requires an analog/RF cancellation signal to avoid saturating the receiver front-end [2], [3], [4]. Full-duplex systems can be broadly categorised into those which generate this analog cancellation signal by directly coupling a replica of transmit signal before the antenna and applying RF signal processing via tapped delay lines, attenuators and phase-shifters e.g., [2], [5]; and those which synthesise the RF cancellation signal from baseband using a separate transmitter chain, e.g., [3], [4], [6], [7] (hereafter referred to as the *Rice* architecture). This paper focuses on the more widely studied Rice architecture, which does not require reconfigurable analog hardware, and allows all signal processing to be performed in the digital baseband [1].

Transmitter non-linearities, in particular those introduced by the RF power amplifier, have a significant impact on full-duplex systems [7], [8], [9]. The analog suppression stage will typically remove the (dominant) components of the self-interference that are proportional to the transmitted signal, i.e.,

the linear terms. The non-linear distortions introduced by non-ideal hardware components remain, and must be removed in the digital domain. Accordingly, much previous theoretical research has focused on developing appropriate models for the distortions introduced by: the digital-to-analog converter (DAC) non-linearities [7]; quantisation noise [9], [10]; IQ imbalance [7], [11]; sampling jitter [12]; phase-noise [13], [14]; and the impact of the physical transmission channel [15]. The RF power amplifier is usually the last component in the transmit chain, and the non-linearities (including memory effects [16]) it introduces [7], [8], [11] will thus cause many of the preceding distortions to couple, complicating the analysis and limiting the effectiveness of models that treat each term in isolation [7], [11].

Unfortunately, for full-duplex to be used in practice high transmit powers are required, e.g., WLAN systems typically operate with 20–30 dBm transmit power. Previous implementations of full-duplex systems employing the Rice architecture have achieved suppression close to the noise-floor for low transmit powers (below 0 dBm) [3], [4]. However, in [3], [4], and [7], operating at higher transmission powers (i.e., outside the linear region of the power amplifiers) was observed to introduce a significant ‘non-cancellable’ residual component. For example, in the hardware setup described by [7], the residual component was 30 dB above the noise-floor when operating with 20 dBm transmit power.

Digital predistortion of the signal before the power amplifier can be used to reduce unwanted out of band transmissions, improve the error vector magnitude at the receiver, and increase efficiency (by allowing operation with lower back-off) [17, pp. 190–196]. Predistortion effectively linearises the output of the power amplifier (and thus of the transmitted RF signal). Accordingly, predistortion may be useful in a full-duplex context by reducing the coupling between the IQ imbalance (and other hardware non-idealities) and the RF non-linear effects. The resulting transmit signal should have significantly reduced non-linear components, which in turn would allow simpler cancellation models to be used.

*Contributions:* In this paper we propose an extension of the Rice full-duplex architecture by including wideband digital predistortion of the transmit chain to account for non-linearities arising from the power amplifier. The cancellation chain is also predistorted to further compensate for any residual non-linear components still present in the transmitted signal. The digital predistortion algorithm is based on a memory polynomial model and multiple iterations are used to improve

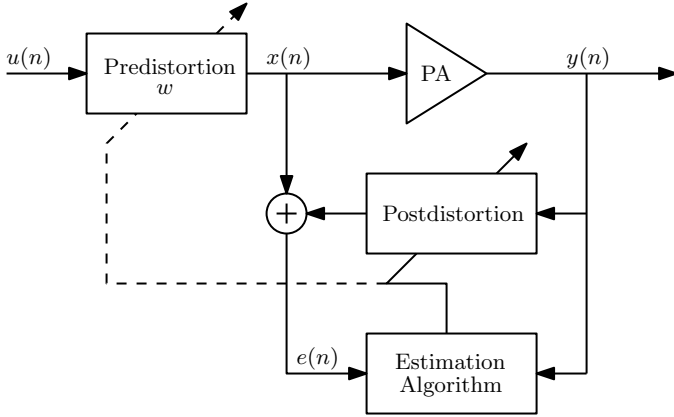


Fig. 1. Application of the predistortion coefficients,  $w$ , to the baseband signal,  $u(n)$ . A postdistortion step is used to estimate  $w$  from training data. Adapted from [18].

convergence. The proposed architecture is implemented on a hardware testbed and experiments are performed to quantify the improvement in suppression that is obtained, relative to the case when no predistortion is applied.

*Outline:* This paper is organised as follows. Section II outlines the methodology for the predistortion of power amplifiers, and includes experimental results when the power amplifier is considered in isolation. Section III discusses how predistortion can be incorporated into a full-duplex system. Implementation results on an experimental testbed are reported in section IV.

## II. POWER AMPLIFIER DIGITAL PREDISTORTION

In this section we outline the application of digital predistortion to a RF power amplifier in isolation; in sections III and IV we discuss how this approach can be extended to full-duplex systems. The basic idea behind digital predistortion is to compensate for the compression introduced by the power amplifier by appropriately distorting the baseband signal. Fig. 1 shows how a baseband signal,  $u(n)$ , is predistorted before passing through the power amplifier. In the ideal case, when the predistorted signal,  $x(n)$ , is applied as an input to the non-linear power amplifier, the output,  $y(n)$ , will simply be  $u(n)$ , and free of non-linear distortion. The predistortion step thus requires finding a suitable model for the *inverse* of the power amplifier. For narrowband signals, where memory effects can be neglected, the inverse can be found relatively easily by sweeping the input power, and either fitting a low-order polynomial model, or deriving look-up-tables [17, pp. 99–101]. However, wideband signals typically require taking the non-linear memory effects into account (which arise from propagation delays in the circuit and thermal time constants [18]), i.e., the output depends not only on the current input but also on the previous values [17].

### A. Memory Polynomial Models

General models for characterising non-linearities with memory can be formulated from the Volterra series [18], [19]. For signals where the bandwidth is small compared to the

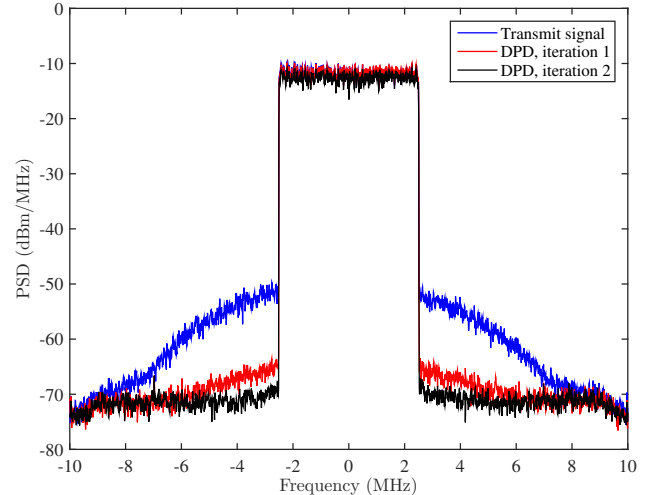


Fig. 2. Spectrum of a 512-tone, 5 MHz OFDM signal through an RF power amplifier (with 20 dBm total output power and 2.48 GHz carrier frequency) and after two successive DPD stages. The signal is attenuated by 20 dB before measurement.

carrier frequency (e.g., in most typical wireless systems), the generalised Volterra series can be simplified to a memory polynomial expansion [18], [20]. In this case, for an arbitrary non-linearity excited with input  $x(n)$ , the output signal,  $y(n)$ , can be expressed

$$y(n) = \sum_{k=0}^{K-1} \sum_{m=0}^{M-1} a_{km} x(n-m) |x(n-m)|^k \quad (1)$$

where  $a_{km}$  are the coefficients to be determined, and  $K$  and  $M$  are the maximum polynomial order and delay considered, respectively. The basis functions in (1) have the form  $x(n) |x(n)|^k$  to ensure the phase-information in  $x(n)$  is preserved. Memory polynomial models have previously been shown to accurately characterise the non-linear effects of a range of RF power amplifiers [18], [21]. Even ordered terms are included in (1) as previous research has shown the DAC introduces baseband non-linear effects [4].

Predistorting for the power amplifier non-linearities requires us to find the inverse of (1). While the inverse of a memory polynomial is also a memory polynomial, explicitly inverting the model is challenging [18], [19]. In this paper, we follow the approach outlined in [18] and [19], where (1) is applied to model the inverse of the power amplifier directly, i.e., the output,  $y(n)$ , is used to predict the input,  $x(n)$ . This method is termed postdistortion, and Fig. 1 depicts a block diagram showing how the coefficients are estimated from the inverse amplifier model. Once the system has converged the coefficients are copied into the predistortion stage, which can then be run in open loop [18].

The  $KM$  predistortion coefficients,  $w$ , are estimated by transmitting a frame (containing  $N$  samples) of training data,  $x = u(n)$ , for  $n = 1, \dots, N$ . The received samples,  $y(n)$ , are gathered into an  $N \times (KM)$  matrix,  $\mathbf{Y}$ . Each column in  $\mathbf{Y}$  corresponds to a specific coefficient in  $w$ , and is distorted according to the basis function,  $y(n-m) |y(n-m)|^k$ . The

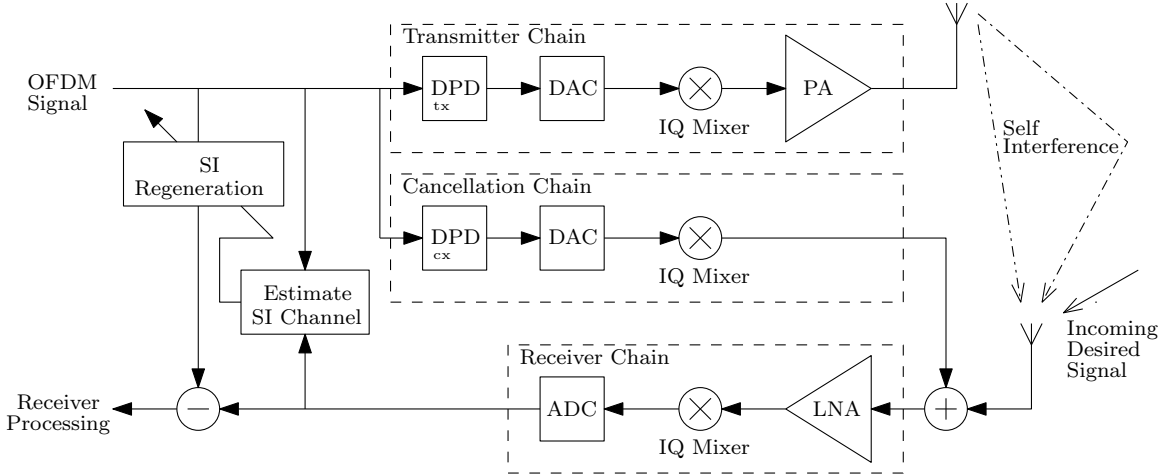


Fig. 3. Full duplex system block diagram showing the transmitter, cancellation and receiver chains. Digital predistortion (indicated by the DPD blocks) is applied to both the transmit and cancellation chains. Further suppression is achieved by estimating and regenerating the self-interference (SI) in the digital domain.

inverse model for the power amplifier can then be compactly expressed as  $\hat{\mathbf{x}} = \mathbf{Y}\mathbf{w}$ . The estimation error is  $\mathbf{e} = \mathbf{x} - \hat{\mathbf{x}}$ , and the least-squares solution that minimises  $\|\mathbf{e}\|^2$  is thus

$$\mathbf{w} = (\mathbf{Y}^H\mathbf{Y})^{-1}\mathbf{Y}^H\mathbf{x}. \quad (2)$$

In practice, the received signal,  $y(n)$ , must first be aligned to  $x(n)$ , but this can be achieved via standard frame-synchronisation techniques.

### B. Experimental Verification

Fig. 2 shows the measured baseband signal spectrum for a wideband orthogonal frequency division multiplex (OFDM) signal after passing through an external Skyworks SE2576L 30 dB gain power amplifier, operating at 2.4 GHz carrier frequency. The OFDM signal has 512 tones (each modulated with 64-QAM) and 5 MHz bandwidth, however, the received signal is sampled at 20 MHz to observe the effectiveness of predistortion on the out-of-band components. The power amplifier is operated with an average output power of 20 dBm (the peak-to-average power ratio of this OFDM signal is approximately 10 dB), and a 20 dB attenuator is placed before the receiver front-end. The RF front-end is a National Instruments NI 5791 transceiver module, and the digital baseband samples are generated and processed using Matlab (further details of the experimental setup are described in section IV). The receiver noise-floor for these measurements is approximately  $-58$  dBm, as the reference level is placed at  $+8$  dB and the ADC has approximately 11.5 effective number of bits, providing 66 dB dynamic range [22].

The wideband OFDM signal is distorted by the power amplifier (other distortions will also be introduced, including IQ imbalance, but we focus here on the amplifier distortions). Fig. 2 shows that when the input signal is not predistorted, strong out-of-band emissions are observed in the received signal spectrum, and the peak of these side-lobes are approximately 40 dB down from the average power level. Also shown in Fig. 2 is the signal spectrum when the same input

signal is digitally predistorted using the approach outlined in section II-A. The maximum delay considered is  $M = 8$ , with maximum polynomial order  $K = 8$ , leading to a total of 81 coefficients to be estimated. The length of the training frame is 41600 samples. In this case, further increasing  $M$ , or  $K$ , does not provide a significant improvement to the residual side-lobe level. After two iterations, the power of the out-of-band emissions can be rejected by 20 dB, and these are only slightly above the noise floor. In order to characterise the non-linearities it is necessary to sample the received signal at a higher frequency than the nominal transmit bandwidth. For example, in Fig. 2, sampling at 5 MHz would lead to the out of band emissions being aliased back in band, complicating the extraction of the predistortion coefficients.

### III. APPLICATION TO FULL-DUPLEX SYSTEMS

In a typical Rice-architecture full-duplex system, the transmission and cancellation chains are sounded to determine the necessary relative delay and attenuation that must be applied to the baseband cancellation signal to align it with the received self-interference [3], [4]. In the absence of non-linear effects and other hardware non-idealities (typically when operating at low transmit power, e.g., below 0 dBm), this approach works well and can provide cancellation close to the noise-floor [4], [7]. However, increasing the transmission power tends to introduce strong non-linear components in the transmitted signal, making it difficult to suppress all the self-interference with an analog cancellation signal. Furthermore, the cancellation chain itself also introduces non-linearities, which arise from the internal amplifiers in the RF front-end (not depicted in Fig. 3). In theory, these non-linear components can be suppressed in the digital domain, however, the cascade of DAC non-linearities, IQ imbalance and RF non-linearities complicates the signal models [7]. In particular, care must be taken not to over-fit any digital models to the analog residual, as in reality the incoming desired signal would also be present.

As shown in Fig. 3, the approach taken in this paper is to predistort both the transmitter and cancellation chains,

thereby accounting for both sets of non-linearities. The impact of the channel (including any internal reflections within the system, and the actual multipath wireless channel) will also be captured by the memory terms of the predistortion model, when sufficient delay terms are included.

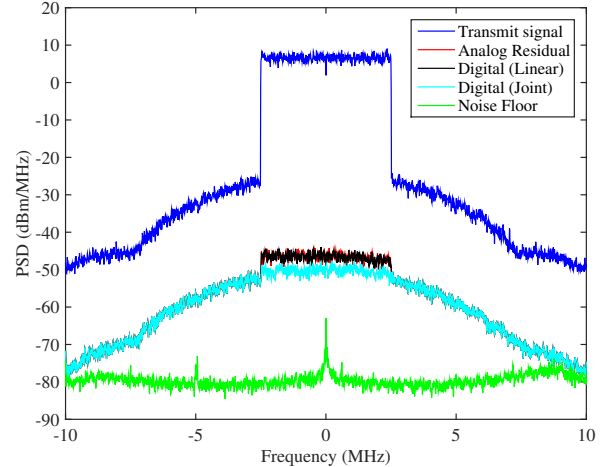
The transmitter and cancellation predistortion coefficients are computed sequentially by sounding the channels using a randomly generated OFDM training signal. First, the transmit-chain coefficients,  $\mathbf{w}_{tx}$ , are computed using (2), where  $\mathbf{Y}$  is the received signal matrix, and  $\mathbf{x}$  is the  $N \times 1$  vector of training samples. The cancellation chain coefficients,  $\mathbf{w}_{cx}$ , could be computed similarly, however, section II-B shows residual non-linearities are present in the received signal even after several iterations of the predistortion algorithm. Thus, to further increase the cancellation, we compute  $\mathbf{w}_{cx}$  by setting  $\mathbf{x}$  in (2) to  $-\mathbf{y}_{tx}$ , the signal obtained after predistorting the transmitter-chain. While computing the coefficients can be computationally expensive (requiring the inverse of a  $81 \times 41600$  matrix), our experiments have shown both sets of coefficients remain largely constant, and thus could be computed off-line and stored.

#### IV. EXPERIMENTAL VERIFICATION

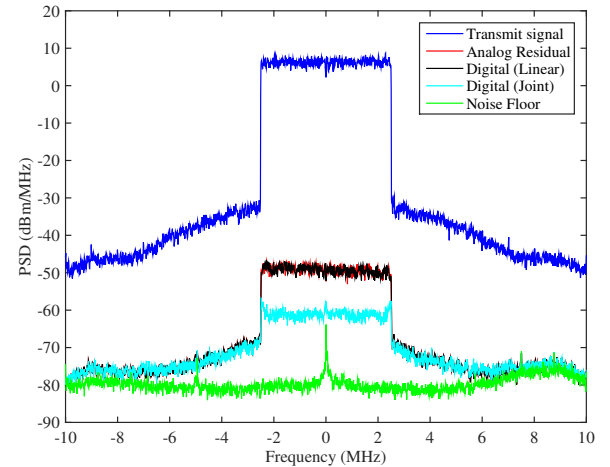
Our full-duplex testbed consists of a NI FlexRIO PXIe-1082 chassis and two NI 5791 transceiver modules, each containing a transmit and receive chain. The same local oscillator is inherently used by the transmit and receive chains within each NI 5791 module and is explicitly shared between each card to reduce the impact of phase noise [13], [14]. An external power amplifier (Skyworks SE2576L) is used to provide up to 20 dBm (average) transmit power, while a low-noise-amplifier (Minicircuits ZX60-272LN+) is used on the receiver side to increase the sensitivity to the incoming desired signal. Two vertically orientated 2.4 GHz ‘rubber duck’ antennas are used and spaced 30 cm apart, providing approximately 20 dB ‘passive’ isolation. As shown in Fig. 3, the RF cancellation signal is applied before the LNA using an RF combiner (Minicircuits ZX10-2-252-S+).

Fig. 4(a) shows the transmitted and residual self-interference spectra for a 5 MHz, 512-tone OFDM signal when no pre-distortion is applied. The (average) transmission power is 20 dBm, and strong side-lobes are observed; these are also present in the residual after analog suppression has been applied. The power of the self-interference before the analog cancellation stage (at the receiving antenna) is approximately 0 dBm; in this case, the analog stage provides 37 dB suppression. Applying linear digital cancellation (i.e., attempting to remove components in the residual proportional to the transmitted signal) does not increase the suppression. This observation is consistent with [3] and [4], where it was noted that the combined suppression obtained from successive analog and digital-linear stages is approximately constant.

As observed in Fig. 4(a), application of a joint cancellation model [7] that includes non-linear components of the complex conjugate of the baseband transmit signal—thereby partially accounting for the IQ imbalance in the mixers, and non-linearities introduced by the DAC—marginally improves the



(a)



(b)

Fig. 4. Experimentally measured suppression spectrum for a 5 MHz bandwidth, 2.48 GHz full-duplex system operating with 20 dBm transmit power: (a) no predistortion applied; and (b) the transmit and cancellation chains are predistorted.

suppression. However, the resulting residual is still approximately 30 dB from the measured noise-floor. In this configuration, the measured noise-floor is approximately  $-68$  dBm (it should be noted that this value is measured after the LNA, which provides approximately 13 dB gain).

Fig. 4(b) shows that predistorting the transmit and cancellation chains results in significantly reduced side-lobes in the analog residual signal. The power of the analog residual is 2 dB lower in the non-predistorted case, however, in this case, application of digital cancellation (using the joint model) significantly reduces the self-interference by a further 11 dB, to within approximately 17 dB of the measured noise floor. To understand why this occurs, let us consider the case where the transmit signal before the power amplifier,  $x(n)$ , is distorted by IQ imbalance,

$$x(n) = \alpha x'(n) + j\beta \tilde{x}'(n), \quad (3)$$

where  $\alpha$  and  $\beta$  are introduced by the gain and phase mismatch

between the I and Q mixers,  $x'(n)$  is the baseband transmit signal, and  $\tilde{x}'(n)$  is the complex conjugate. Substituting (3) into (1), gives the resulting coupling of IQ imbalance and RF non-linear terms in the transmitted signal,

$$y(n) = \sum_{k=0}^{K-1} \sum_{m=0}^{M-1} a_{km} \left( \alpha x'(n-m) + j\beta \tilde{x}'(n-m) \right) \left| \alpha x'(n-m) + j\beta \tilde{x}'(n-m) \right|^k. \quad (4)$$

Non-linear components of the complex conjugate are present in (4), and these will not be removed by the analog cancellation stage. The residual self-interference is difficult to suppress digitally, as shown in Fig. 4(a), due to the large number of non-linear cross-terms containing both  $x'(n)$  and  $\tilde{x}'(n)$  [7]. However, predistorting for the power amplifier, essentially ‘undoes’ the coupling in (4), reducing the relative strength of the cross-terms, leaving only the linear IQ terms, which can easily be removed in the digital stage.

Compared to Fig. 2, stronger out of band emission are observed in the transmit signal spectra shown in Fig. 4(b). However, it must be noted that in Fig. 4(b), the transmit signal is measured *before* the transmitting antenna using a coupler. The predistortion applied to the transmitted signal also accounts for delays in the wireless channel and any further non-linearities introduced by the receiver chain. It should also be noted that in Figs. 4(a) and (b), the digital cancellation models are only fit to the first 10% of the analog residual signal to avoid the risk of over-fitting. The computed coefficients are then applied to the remainder of the frame to determine the suppression achieved. The actual transmission frame is also different from the those used to sound the channel or compute the predistortion coefficients.

## V. CONCLUSIONS

One of the most significant limitations in the practical realisation of full-duplex systems are the non-linearities introduced by the RF power amplifier. In particular, for wideband transmission, the non-linear memory effects of the power amplifier cascade and couple with preceding distortions introduced by non-ideal hardware components. In this paper we propose digital predistortion of the transmitter-chain to linearise the power amplifier. Implementation results show that by doing so, many of the other hardware impairments, such as IQ imbalance, can be easily suppressed in the digital domain. For a 20 dBm OFDM signal operating with 5 MHz bandwidth, our results show a further 13 dB suppression can be obtained, compared to the case when predistortion is not applied.

## REFERENCES

- [1] A. Sabharwal, P. Schniter, D. Guo, D. Bliss, S. Rangarajan, and R. Wichman, “In-band full-duplex wireless: Challenges and opportunities,” *IEEE J. Sel. Areas Commun.*, vol. 32, no. 9, pp. 1637–1652, 2014.
- [2] M. Jain, J. I. Choi, T. Kim, D. Bharadia, S. Seth, K. Srinivasan, P. Levis, S. Katti, and P. Sinha, “Practical, real-time, full duplex wireless,” in *Proc. 17th International Conference on Mobile Computing and Networking*. ACM, 2011, pp. 301–312.
- [3] M. Duarte, C. Dick, and A. Sabharwal, “Experiment-driven characterization of full-duplex wireless systems,” *IEEE Trans. Wireless Commun.*, vol. 11, no. 12, pp. 4296–4307, 2012.

- [4] A. Balatsoukas-Stimming, P. Belanovic, K. Alexandris, and A. Burg, “On self-interference suppression methods for low-complexity full-duplex MIMO,” in *Asilomar Conference on Signals, Systems and Computers*, 2013, pp. 992–997.
- [5] D. Bharadia, E. McMillin, and S. Katti, “Full duplex radios,” in *Proc. ACM Conference on SIGCOMM*, 2013, pp. 375–386.
- [6] M. Duarte, A. Sabharwal, V. Aggarwal, R. Jana, K. Ramakrishnan, C. Rice, and N. Shankaranarayanan, “Design and characterization of a full-duplex multi-antenna system for WiFi networks,” *IEEE Trans. Veh. Technol.*, vol. 63, no. 3, pp. 1160–1177, 2014.
- [7] A. Balatsoukas-Stimming, A. C. M. Austin, P. Belanovic, and A. P. Burg, “Baseband and RF hardware impairments in full-duplex wireless systems: experimental characterisation and suppression,” *EURASIP Journal on Wireless Communications and Networking*, vol. 2015, no. 142, 2015.
- [8] S. Li and R. Murch, “An investigation into baseband techniques for single-channel full-duplex wireless communication systems,” *IEEE Trans. Wireless Commun.*, vol. 13, no. 9, pp. 4794–4806, 2014.
- [9] D. Korpi, T. Riihonen, V. Syrjala, L. Anttila, M. Valkama, and R. Wichman, “Full-duplex transceiver system calculations: Analysis of ADC and linearity challenges,” *IEEE Trans. Wireless Commun.*, vol. 13, no. 7, pp. 3821–3836, July 2014.
- [10] T. Riihonen and R. Wichman, “Analog and digital self-interference cancellation in full-duplex MIMO-OFDM transceivers with limited resolution in A/D conversion,” in *Asilomar Conference on Signals, Systems and Computers*, 2012, pp. 45–49.
- [11] D. Korpi, L. Anttila, V. Syrjala, and M. Valkama, “Widely linear digital self-interference cancellation in direct-conversion full-duplex transceiver,” *IEEE J. Sel. Areas Commun.*, vol. 32, no. 9, pp. 1674–1687, Sept 2014.
- [12] V. Syrjala and K. Yamamoto, “Is sampling jitter a problem in full-duplex radio transceivers or not?” in *IEEE 79th Vehicular Technology Conference (VTC Spring)*, 2014, pp. 1–5.
- [13] A. Sahai, G. Patel, C. Dick, and A. Sabharwal, “On the impact of phase noise on active cancellation in wireless full-duplex,” *IEEE Trans. Veh. Technol.*, vol. 62, no. 9, pp. 4494–4510, Nov 2013.
- [14] V. Syrjala, M. Valkama, L. Anttila, T. Riihonen, and D. Korpi, “Analysis of oscillator phase-noise effects on self-interference cancellation in full-duplex OFDM radio transceivers,” *IEEE Trans. Wireless Commun.*, vol. 13, no. 6, pp. 2977–2990, June 2014.
- [15] E. Everett, A. Sahai, and A. Sabharwal, “Passive self-interference suppression for full-duplex infrastructure nodes,” *IEEE Trans. Wireless Commun.*, vol. 13, no. 2, pp. 680–694, 2014.
- [16] L. Anttila, D. Korpi, E. Antonio-Rodriguez, R. Wichman, and M. Valkama, “Modeling and efficient cancellation of nonlinear self-interference in MIMO full-duplex transceivers,” in *Globecom Workshops*, 2014, pp. 777–783.
- [17] L. Smaïni, *RF Analog Impairments Modeling for Communication Systems Simulation: Application to OFDM-based Transceivers*. Chichester: Wiley, 2012.
- [18] D. R. Morgan, Z. Ma, J. Kim, M. G. Zierdt, and J. Pastalan, “A generalized memory polynomial model for digital predistortion of RF power amplifiers,” *IEEE Trans. Signal Process.*, vol. 54, no. 10, pp. 3852–3860, Oct. 2006.
- [19] C. Eun and E. J. Powers, “A new Volterra predistorter based on the indirect learning architecture,” *IEEE Trans. Signal Process.*, vol. 45, no. 1, pp. 223–227, Jan. 1997.
- [20] J. Kim and K. Konstantinou, “Digital predistortion of wideband signals based on power amplifier model with memory,” *Electron. Lett.*, vol. 37, no. 23, pp. 1417–1418, Nov. 2001.
- [21] L. Ding, G. Zhou, D. Morgan, Z. Ma, J. Kenney, J. Kim, and C. Giardinà, “A robust digital baseband predistorter constructed using memory polynomials,” *IEEE Trans. Commun.*, vol. 52, no. 1, pp. 159–165, 2004.
- [22] “Texas Instruments ADS4246 datasheet,” <http://www.ti.com/lit/ds/symlink/ads4246.pdf>.